Journal of Bioinformatics and Computational Biology
Vol. 14, No. 6 (2016) 1650032 (18 pages)

DOI: 10.1142/S0219720016500323

World Scientific
www.worldscientific.com

Global peak alignment for comprehensive two-dimensional gas chromatography mass spectrometry using point matching algorithms

Beichuan Deng[*,¶], Seongho Kim[†,‡,‖], Hengguang Li[*,**], Elisabeth Heath[‡,††] and Xiang Zhang[§,‡‡]

[*]*Department of Mathematics, Wayne State University Detroit, MI, 48201, USA*

[†]*Biostatistics Core, Karmanos Cancer Institute Wayne State University, Detroit, MI 48201, USA*

[‡]*Department of Oncology, School of Medicine Wayne State University Detroit, MI 48201, USA*

[§]*Department of Chemistry, University of Louisville Louisville, KY 46209, USA*

[¶]*beichuan.deng@wayne.edu*
[‖]*kimse@karmanos.org*
[**]*hli@math.wayne.edu*
[††]*heathe@karmanos.org*
[‡‡]*xiang.zhang@louisville.edu*

Received 18 April 2016
Revised 16 August 2016
Accepted 30 August 2016
Published 21 September 2016

Comprehensive two-dimensional gas chromatography coupled with mass spectrometry (GC × GC-MS) has been used to analyze multiple samples in a metabolomics study. However, due to some uncontrollable experimental conditions, such as the differences in temperature or pressure, matrix effects on samples and stationary phase degradation, there is always a shift of retention times in the two GC columns between samples. In order to correct the retention time shifts in GC × GC-MS, the peak alignment is a crucial data analysis step to recognize the peaks generated by the same metabolite in different samples. Two approaches have been developed for GC × GC-MS data alignment: profile alignment and peak matching alignment. However, these existing alignment methods are all based on a local alignment, resulting that a peak may not be correctly aligned in a dense chromatographic region where many peaks are present in a small region. False alignment will result in false discovery in the downstream statistical analysis. We, therefore, develop a global comparison-based peak alignment method using point matching algorithm (PMA-PA) for both homogeneous and heterogeneous data. The developed algorithm PMA-PA first extracts feature points (peaks) in the chromatography and then searches globally the matching peaks in the consecutive chromatography by adopting the projection of rigid and nonrigid transformation. PMA-PA is further applied to two real experimental data sets,

[‖]Corresponding author.

showing that PMA-PA is a promising peak alignment algorithm for both homogenous and heterogeneous data in terms of $F1$ score, although it uses only peak location information.

Keywords: GC-MS; metabolomics; peak alignment; point matching algorithm.

1. Introduction

Multiple samples are usually analyzed in a metabolomics study to obtain a better statistical power, by assessing the biological variation between samples as well as the technical variation generated during sample analysis. Due to some uncontrollable experimental conditions, such as the differences in temperature or pressure, matrix effects on samples, and stationary phase degradation, there is always a shift of retention times in the two gas chromatography (GC) columns between samples. Therefore, the peak alignment is a crucial data analysis step to recognize the peaks generated by the same metabolite in different samples. In order to correct the retention time shifts in the two-dimensional GC system, two approaches have been developed to align comprehensive two-dimensional GC coupled with mass spectrometry (GC×GC-MS) data: profile alignment and peak matching alignment.

Four profile alignment methods have been reported using the two-dimensional retention times: the rank annihilation method,[1] a correlation-optimized shifting method,[2] a piecewise retention time alignment,[3] and a two-dimensional correlation optimized warping.[4] Aligning metabolite peaks solely based on the two-dimensional retention times may introduce a high rate of false-positive alignment because some metabolites with similar chemical functional groups have similar retention times in both GC dimensions. For this reason, four peak matching methods, MSort,[5] DISCO,[6] mSPA,[7] and SWPA [8] were developed using both the two-dimensional retention times and mass spectrum similarity for alignment. The main difference between MSort/mSPA and DISCO/SWPA approaches is that DISCO and SWPA can be applied to both homogeneous and heterogeneous data while MSort and mSPA are only able to align homogeneous data. The homogeneous data mean that all samples were analyzed under the identical experiment conditions and the heterogeneous data refer that experiment data were acquired under different experiment conditions. However, these existing alignment methods are all based on a local alignment, resulting that a peak is likely to be not correctly aligned in a dense chromatographic region where many peaks are present in a small region. False alignment will result in false discovery in the downstream statistical analysis.

Point matching algorithms (PMAs) are often used in the domains of computer vision and medical imaging. It first extracts feature points in the image and then searches globally the matching points in the consecutive images by adopting the projection of rigid and nonrigid transformation. There are several versions of PMA including the iterated closest point (ICP) algorithm,[9] robust point matching (RPM)[10] the thin-plate spline RPM (TPS-RPM),[11] coherent point drift (CPD),[12] etc. The CPD method has two versions: rigid and nonrigid. The rigid CPD is an iterative method based on Gaussian mixture model (GMM), while the nonrigid CPD regularizes the displacement field between the point sets following the motion coherence theory,

optimally computing the transformation. A key advantage of CPD over other PMA methods is the ability to dramatically reduce computational complexity and expense.

To resolve the aforementioned challenges on existing peak alignment algorithms, we develop a global comparison based peak alignment method using PMA (PMA-PA). The developed PMA-PA algorithm employs the CPD method. We choose the CPD method because of the following properties: (i) robustness to degradations such as outliers and missing points, (ii) ability to deal with high dimensional data efficiently and (iii) ability to reduce computational complexity and expense. Note that outliers are the points (peaks) that have no corresponding points (peaks) to align due to missing points in a corresponding data set. That is, outliers and missing points are correspondingly defined. The proposed PMA-PA algorithm can further deal with both homogeneous and heterogeneous data. In this study, we particularly focus on examining the feasibility and ability of PMA-PA in relation to peak alignment using the two-dimensional retention times only.

2. Materials and Methods

2.1. *GC×GC-MS data*

A mixture of 76 compound standards (8270 MegaMix, Restek Corp., Bellefonte, PA), C7–C40 saturated alkanes (Sigma-Aldrich Corp., St. Louis, MO) and a deuterated six component semi-volatiles internal standard (ISTDF) mixture (Restek Corp., Bellefonte, PA) at a concentration of 2.5 μg/mL were analyzed on a LECO Pegasus four-dimensional (4D) GC×GC-MS instrument (LECO Corporation, St. Joseph, MI, USA) equipped with a cryogenic modulator. The GC×GC-MS analyses were repeated 10, 2 and 4 times under three different temperatures, 5°C/min, 7°C/min, and 10°C/min, respectively, resulting in a total of 16 data sets. All GC×GC-MS analyses were performed on a LECO Pegasus 4D time-of-flight mass spectrometer (TOF-MS) with a Gerstel MPS2 autosampler. The Pegasus 4D GC×GC-MS instrument was equipped with an Agilent 7890 gas chromatograph featuring a LECO two-stage cryogenic modulator and secondary oven. A 30 m × 0.25 mm i.d. × 0.25 μm film thickness, Rxi-5 ms GC capillary column (Restek Corp., Bellefonte, PA) was used as the primary column for the GC×GC-MS analysis. A second GC column of 1.2 m × 0.10 mm i.d. × 0.10 μm film thickness, BPX-50 (SGE Incorporated, Austin, TX) was placed inside the secondary GC oven after the thermal modulator. The helium carrier gas flow rate was set to 1.0 mL/min at a corrected constant flow via pressure ramps. A 1 μL liquid sample was injected into the liner using the splitless mode with the injection port temperature set at 260°C. The primary column temperature was programmed with an initial temperature of 60°C for 0.5 min and then ramped at a variable temperature gradient to 315°C. The secondary column temperature program was set to an initial temperature of 65°C for 0.5 min and then also ramped at the same temperature gradient employed in the first column to 320°C accordingly. The thermal modulator was set to +20°C relative to the primary oven, and a modulation time of 5 s was used. The MS mass range was 10–750 m/z with an acquisition rate of 150 spectra per second. The ion source chamber was set at 230°C

with the MS transfer line temperature set to 260°C, and the detector voltage was 1800 V with electron energy of 70 eV. These data sets were previously used for development of DISCO,[6] mSPA,[7] and SWPA[8] algorithms.

2.2. *Sketch of CPD algorithm*

As mentioned above, PMA is a process of finding a spatial transformation that aligns two point sets. Let $\{M, S\}$ be two point sets in a finite-dimensional vector space R^d, which contain l and n points, respectively, i.e. $|M| = l$, $M \subset R^d$, $|S| = n$ and $S \subset R^d$. Note that $d = 2$ in this study. A key procedure of PMA is to find a transformation T to be applied to the moving 'model' point set M such that the difference between M and the static 'scene' set S is minimized, i.e. to find $T_{\min}$:

$$\text{dist}(T_{\min}(M), S) = \min_{T}\{\text{dist}(T(M), S)\}. \tag{1}$$

In this work, we apply the CPD algorithm for both rigid and nonrigid point set registrations, introduced by Myronenko and Song.[12] CPD considers the alignment of two point sets, 'model' and 'scene' sets, as a probability density estimation problem and applies GMMs to both point sets. Then it fits GMM centroids representing the 'model' set to the 'scene' set by maximizing the likelihood, and aligns two point sets using the posterior probabilities of the GMM components. By doing so, it preserves the topological structure of the points sets during the alignment, which is a critical characteristic of CPD. In order to account for outliers and missing points, an extra distribution term, such as large Gaussian[15] or uniform distribution,[16] is included to the GMM components. In the CPD method, a uniform distribution is added to the mixture model to account for outliers and missing points. The GMM probability density function of CPD is as follows:

$$p(\mathbf{x}) = \omega \sum_{m=1}^{M} \frac{1}{M} p(\mathbf{x}|m) + (1-\omega)\frac{1}{N}, \tag{2}$$

where $p(\mathbf{x}|m) = \frac{1}{(2\pi\sigma^2)^{d/2}} \exp - \frac{||\mathbf{x}-\mathbf{y_m}||^2}{2\sigma^2}$, and ω is a weight between 0 and 1. Then CPD reparametrizes the GMM centroid location by a set of parameters θ and ω, and fits the two density functions together by maximizing the likelihood, or equivalently, by minimizing the negative log-likelihood function

$$E(\theta, \omega^2) = -\sum_{n=1}^{N} \log(p(\mathbf{x_n}|m)) \tag{3}$$

under the assumption that the data are independently and identically distributed.

To estimate θ and ω, the expectation–maximization (EM) algorithm is used.[14] The initial θ_0 and ω_0 are guessed and plugged into the log likelihood function, $E(\theta_0, \omega_0^2)$ in the E-step. Then, in the M-step, according to the Bayes' Theorem, the new parameters θ_1 and ω_1 are found by minimizing the expectation of the

log-likelihood function

$$Q = -\sum_{n=1}^{N}\sum_{m=1}^{M} P_0(m|\mathbf{x_n}) \log(p_1(\mathbf{x_n}|m)) \tag{4}$$

where the indices correspond to the indices of the parameters. In the rigid case, CPD imposes the coherence constraint by reparametrization of GMM centroid locations with rigid parameters and derive a closed form solution of the maximization step of the iteration. In the nonrigid case, it imposes the coherence constraint by regularizing the displacement field and using the variational calculus to derive the optimal transformation. For more details, we refer the reader to the work of Myronenko and Song.[12]

2.3. *Z-score standardization*

The domains of the first and the second dimension retention times in GC×GC-MS data are different from each other. For instance, the first dimension retention time ranges from 300s to 4000s, while the second dimension retention time ranges 0s to 5s. This discrepancy often hampers accurate peak alignment, in particular, for the heterogeneous case. To resolve this difficulty, we use the z-score that is a common method to standardize a variable. It is defined as

$$X_z = \frac{X - E(X)}{\sigma(A)}, \tag{5}$$

where $E(X)$ and $\sigma(A)$ are the expectation and its standard deviation of the variable X, respectively. We apply z-score to precondition the data sets.

2.4. *PMA-PA algorithm*

The developed PMA-PA algorithm aligns the two sets of peaks generated from two GC×GC-MS experiments by the CPD method. However, the CPD method finds the transformation of the 'model' data set only, resulting that the aligned results are not consistent with the choice of the 'model' data set. Therefore, to produce the consistent aligned peak pairs regardless of the choice of the 'model' data set, the PMA-PA performs the CPD alignment two times by switching the role of the 'model' and the 'scene' data sets. Then the consensus is carried out to preserve the peak pairs only that are present in both CPD-based aligned lists.

2.5. *Performance evaluation*

To reflect the real systemic biases generated from GC×GC-MS experiments, we employed the real experiment data sets and used the compound names identified at each data set to evaluate the performance of the developed PMA-PA algorithms. That is, if the aligned peaks (points) have the same compound name, we consider this matching as a positive matching pair. If not, this matching will be considered as a negative matching pair.

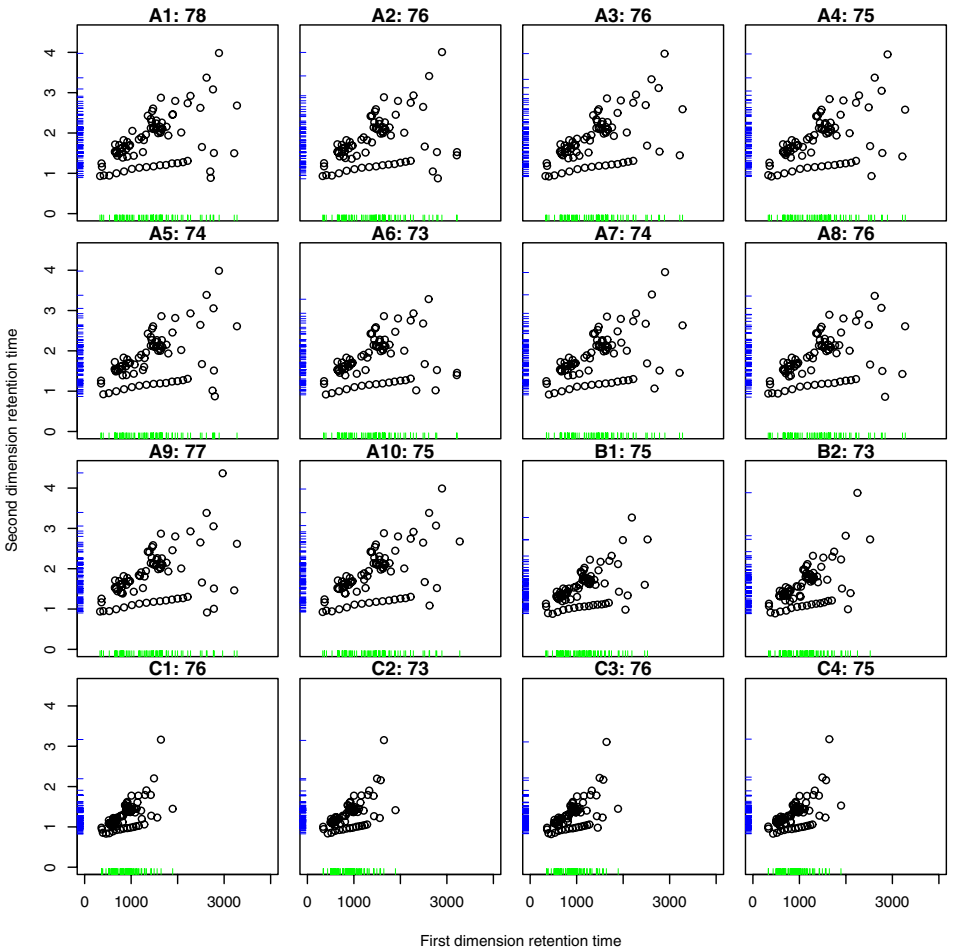

Fig. 1. Chromatograms of the first spiked-in data set. A1–A10: under 5°C/min, B1–B2: under 7°C/min, and C1–C4: under 10°C/min. The numbers indicate the number of compounds identified and the rug plot represents the density of each retention time.

In particular, as described before, the first data set of 16 experiments was generated by the mixture of compound standards, meaning that these compounds were artificially introduced in the samples. As shown in Fig. 1, most of these compound standards were detected and correctly identified from each experimental data set. Furthermore, to reflect the heterogeneous cases, the experiments were carried out under three different temperatures, 5°C/min, 7°C/min, and 10°C/min. The peak alignments within the same temperatures represent the homogeneous alignment, while those between the different temperatures represent the heterogenous alignment. In addition to the data acquired from mixture of compound standards, the real biological data were used to reflect a dense chromatographic region where many peaks are present in a small region as can be seen in Fig. 2. Since these data were

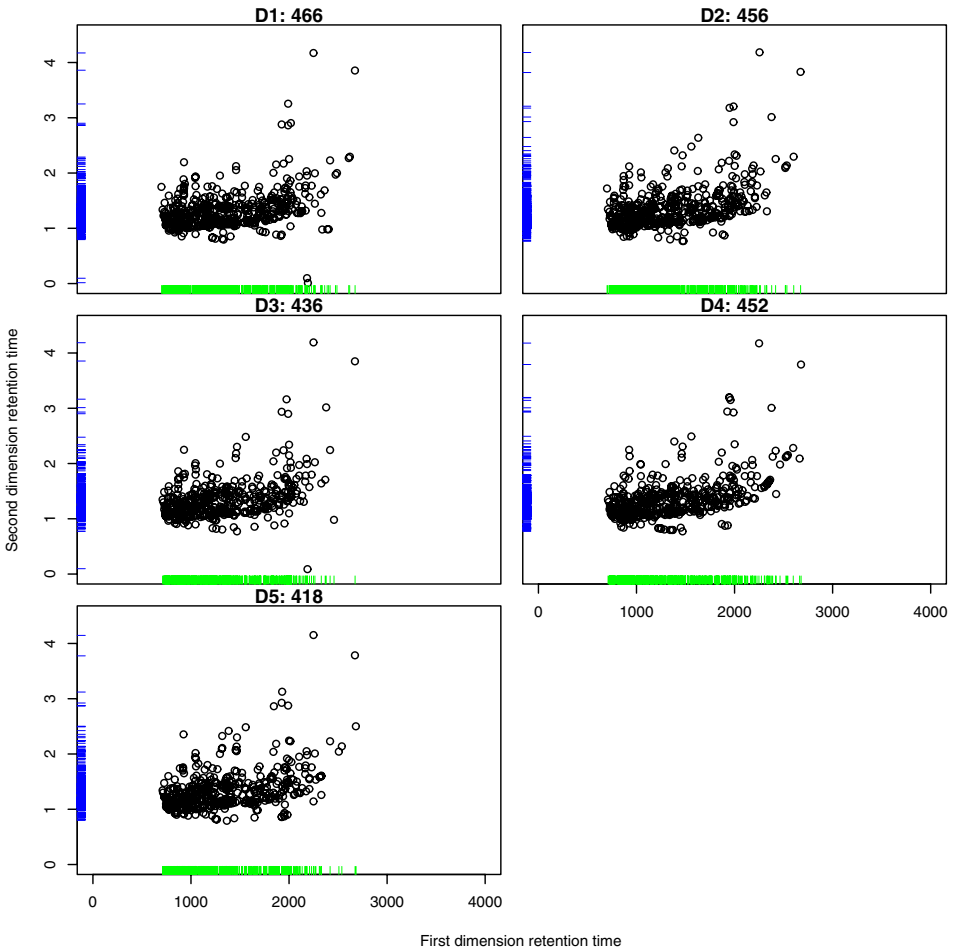

Fig. 2. Chromatograms of five GC×GC-MS data set acquired from metabolite extracts of mouse livers. The numbers indicate the number of compounds identified and the rug plot represents the density of each retention time.

carried out under the same experimental conditions, the peak alignments among these biological data reflect the homogeneous alignment.

Suppose that there are l points in the 'model' set $M = \{m_1, m_2, \ldots, m_l\}$, and n points in the 'scene' set $S = \{s_1, s_2, \ldots, s_n\}$, with u positive matching pairs $\{(m_{i_1}, s_{j_1}), (m_{i_2}, s_{j_2}), \ldots, (m_{i_u}, s_{j_u})\}$, where $u \leq \min(l, n)$. If a certain point matching method is applied to the two data sets, M and S, and v matched pairs are found, then the true positive rate (TPR) and predictive positive value (PPV) are defined as follows:

$$\text{TPR} = \frac{\text{TP}}{u}; \quad \text{PPV} = \frac{\text{TP}}{v}, \tag{6}$$

where TP is the number of positive matching pairs that were aligned as positive (true positive) and is less than or equal to $\min(u, v)$. The $F1$ score is defined as the harmonic average of TPR and PPV, i.e.

$$F1 \text{ score} = \frac{2 \cdot \text{TPR} \cdot \text{PPV}}{\text{TPR} + \text{PPV}}. \tag{7}$$

2.6. *Tuning parameters*

The CPD method has two types of transformation: rigid and nonrigid transformation. The rigid transformation requires the three tuning parameters: maximum step, tolerance, and $\omega \in [0, 1)$, while the nonrigid transformation has two more tuning parameters in addition to those of the rigid transformation: maximum step, tolerance, $\omega \in [0, 1)$, $\beta \in [1, 5]$ and $\lambda \in [1, 5]$. The first two tuning parameters, maximum step and tolerance, control when to stop the EM iteration. The third parameter ω plays a role in preconditioning the amount of the potential outliers/missing points in the data sets. As can be seen in Eq. (2), the smaller ω, the more outliers/missing points because the uniform distribution will have more weights as the ω decreases. The parameter β in the nonrigid transformation represents the width of smoothing Gaussian filter,[13] i.e. the less β, the less oscillations (high frequency waves), resulting in the transformation function smoother. The last parameter λ tunes the weight of the penalty term, i.e. as λ decreases, the likelihood function becomes dominated, while as λ increases, the objective function becomes smoother. According to our application to real experiment data sets, the tuning parameters, maximum step and tolerance, barely affect the result. However, the parameter ω plays a critical role in improving the performance of both rigid and nonrigid methods, and β and λ need only for the nonrigid algorithm. We also consider the two more factors that affect the performance of peak alignment, which are the z-score standardization and the rigid/nonrigid transformations.

In case of the rigid transformation, we explore the effect of ω on the peak alignment by taking 10 points by dividing the interval $[0, 0.999]$ into nine equal-width subintervals. Similarly, in case of the nonrigid transformation, we evaluate the influence of ω, β and λ on the peak alignment by taking 10 cut-points for each interval of the three tuning parameters.

3. Implementations

3.1. *Homogeneous cases*

The developed PMA-PA algorithms are applied to the homogeneous data sets A1–A10 and the performance results are depicted in Fig. 3. The rigid method without z-score is the most sensitive to the tuning parameter ω, while the nonrigid without z-score has little influence on the change of ω. The methods with z-score show the similar behavior in regard to ω. The best performance occurs when the rigid

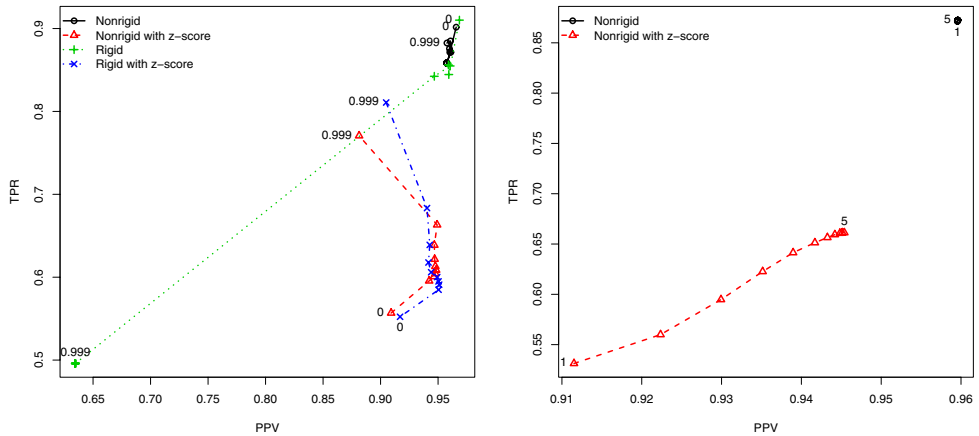

(a) ω

(b) β

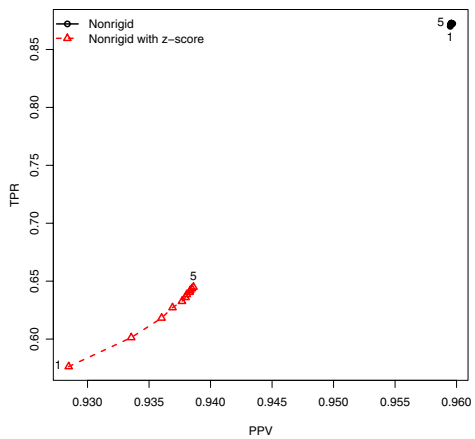

(c) λ

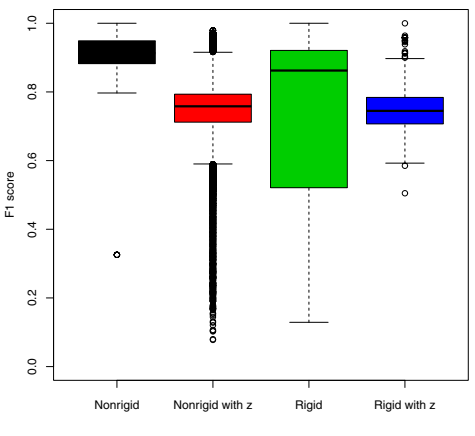

(d) $F1$ score

Fig. 3. Homogeneous case using the data sets A1–A10.

without z-score is applied with ω of 0 in terms of the PPV-TPR plot. Note that the best performance will occur when the point is located in the top right-most area in the PPV-TPR plot.

The nonrigid method has two more tuning parameters, β and λ. Both plots (Figs. 3(b) and 3(c)) clearly show that there is no effect of β and λ on the method without z-score, but their influence on the method with z-score is not ignorable. The nonrigid method without z-score outperforms that with z-score when β and λ are considered.

The overall performance in homogeneous cases is displayed in Fig. 3(d) in terms of $F1$ score. As shown in other figures, the variance of the nonrigid method without z-score is the smallest among others and the rigid method without z-score has the

Table 1. The overall mean $F1$ score for each of pairwise peak alignment results.

M	z	N	$F1$ score	N	$F1$ score	N	$F1$ score
		Homogeneous		Heterogeneous		Mice	
NR	No	54450	0.9134 (0.0002)	48400	0.0173 (0.0001)	12100	0.4134 (0.0005)
NR	Yes	54450	0.7471 (0.0004)	48400	0.5957 (0.0005)	12100	0.2105 (0.0008)
R	No	450	0.7305 (0.0114)	400	0.0143 (0.0007)	100	0.1819 (0.0201)
R	Yes	450	0.7492 (0.0033)	400	0.5338 (0.0045)	100	0.1860 (0.0066)

Note: 'M' stands for 'Method'; 'NR' and 'R' represent the nonrigid and rigid transformations, respectively; 'z' stands for the z-score standardization; 'N' is the total number of pairs considered; the numbers in parentheses represent the standard error.

largest variance. The ANOVA followed by Tukey's post hoc tests demonstrates that the nonrigid without z-score significantly achieves the highest mean $F1$ score compared to other methods as shown in Table 1. The cases with the maximum $F1$ score are further shown in Table 2. Interestingly, the maximum $F1$ score occurs when the rigid without z-score is used with $\omega = 0$, although it is not significantly different from when the nonrigid without z-score is used with $\omega = 0$, $\beta = 5$ and $\lambda = 2.2$.

3.2. *Heterogeneous cases*

The results of the heterogeneous cases are shown in Fig. 4. In this case, we aligned two sets of experiment data that were generated in different temperatures, i.e. (A and B), (A and C) and (B and C), using PMA-DA.

Table 2. The cases with the maximum $F1$ score for each of pairwise peak alignment results.

M	z	N	ω	β	λ	TPR	PPV	$F1$ score
						Homogeneous		
NR	No	45	0	5	2.2	0.9061 (0.0065)	0.9688 (0.0039)	0.9361 (0.0049)
NR	Yes	45	0.999	1.8	1	0.8045 (0.0130)	0.9278 (0.0070)	0.8609 (0.0104)
R	No	45	0			0.9101 (0.0066)	0.9686 (0.0041)	0.9382 (0.0052)
R	Yes	45	0.999			0.8108 (0.0167)	0.9049 (0.0109)	0.8543 (0.0142)
						Heterogeneous		
NR	No	40	0.999	1	1	0.0192 (0.0029)	0.0446 (0.0070)	0.0268 (0.0041)
NR	Yes	40	0.889	2.2	5	0.5765 (0.0094)	0.9136 (0.0044)	0.7057 (0.0081)
R	No	40	0.111			0.0144 (0.0016)	0.0410 (0.0044)	0.0212 (0.0023)
R	Yes	40	0.889			0.4527 (0.0104)	0.7776 (0.0128)	0.5717 (0.0115)
						Mice		
NR	No	10	0.999	1	1	0.5222 (0.0217)	0.4515 (0.0142)	0.4840 (0.0172)
NR	Yes	10	0.555	4.6	2.6	0.2261 (0.0065)	0.4593 (0.0129)	0.3028 (0.0082)
R	No	10	0.778			0.2230 (0.0725)	0.1948 (0.0612)	0.2078 (0.0663)
R	Yes	10	0.999			0.3186 (0.0363)	0.2965 (0.0268)	0.3068 (0.0311)

Note: 'M' stands for 'Method'; 'NR' and 'R' represent the nonrigid and rigid transformations, respectively; 'z' stands for the z-score standardization; 'N' is the total number of pairs considered; The numbers in parentheses represent the standard error.

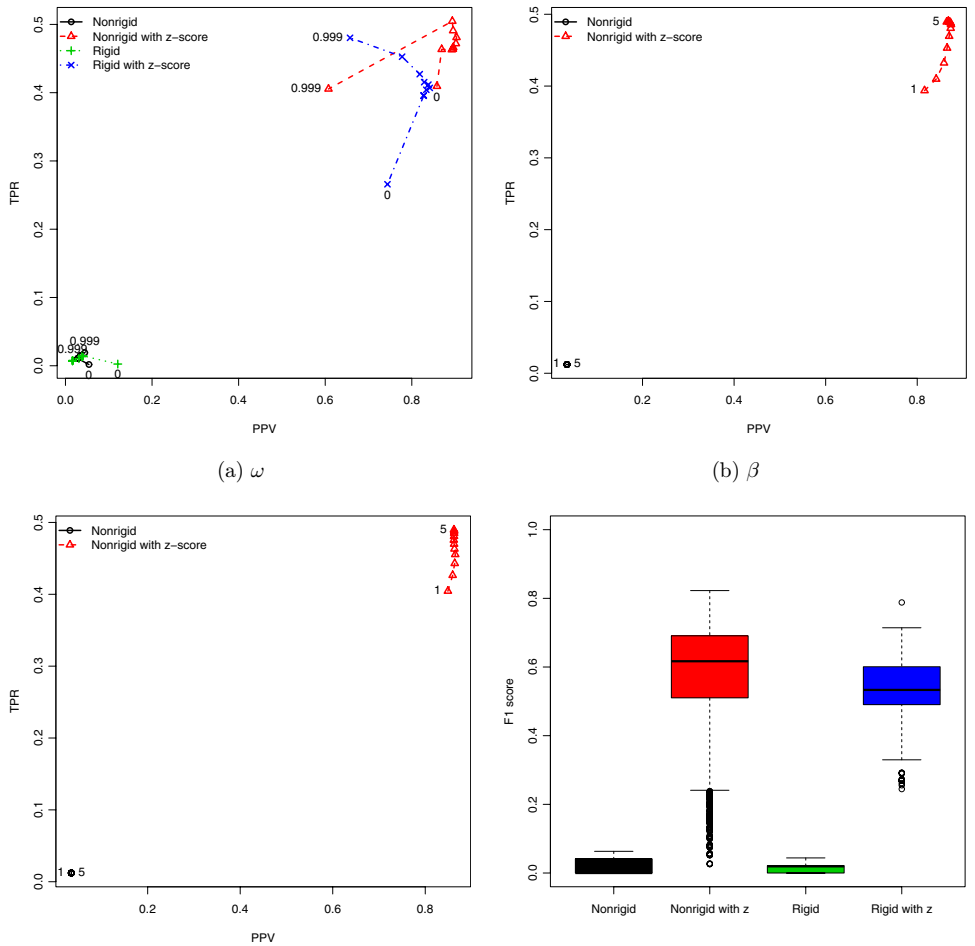

(a) ω (b) β

(c) λ (d) $F1$ score

Fig. 4. Heterogeneous case using the data sets A1–A10:B1–B2:C1–C4.

As expected, we can see that its performance is quite different from that of the homogeneous cases. Although the effect of ω is little to the methods without z-score similar to the homogeneous cases, the peak alignment performs much better with the methods with z-score. Likewise, the effects of β and λ are relatively large in the nonrigid method with z-score, but it outperforms the nonrigid method without z-score in terms of the PPV-TPR plot.

As can be seen in Fig. 4(d), the influence of tuning parameters on peak alignment is smaller without z-score, but the overall performance is much better with z-score than that without z-score. In terms of the overall mean $F1$ score (see Table 1), both methods with z-score achieve comparable peak alignments, but the one-way ANOVA with Tukey's post hoc analysis confirms that the nonrigid method with

z-score has significantly higher mean of $F1$ scores than others. The maximum $F1$ score is observed when the nonrigid method with z-score is applied with $\omega = 0.889$, $\beta = 2.2$, and $\lambda = 5$, as shown in Table 2.

3.3. *Analysis of biological data*

The real biological data sets (D1–D5) are more dense than the data sets A, B and C, as displayed in Fig. 2. The developed algorithms are applied to these biological data sets and its results are displayed in Fig. 5.

Similar to the previous cases, the nonrigid method without z-score shows the least sensitive to the tuning parameters. In case of ω, the rigid method with z-score can

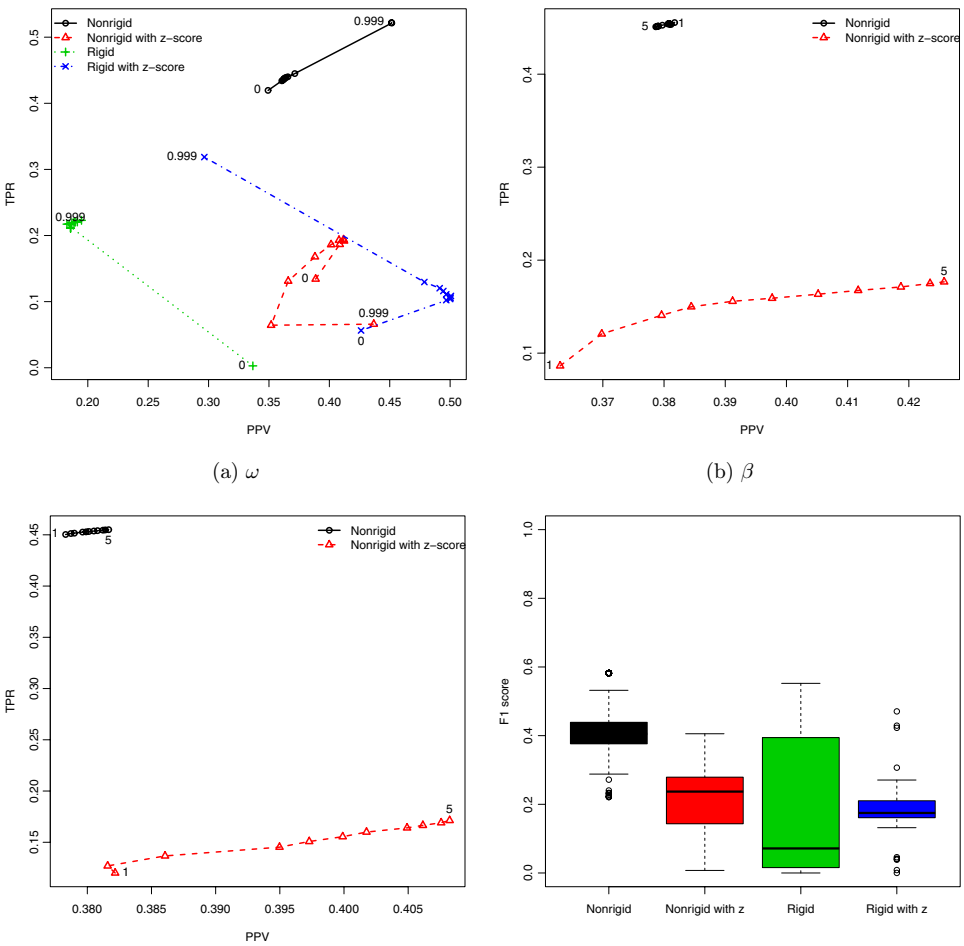

(a) ω (b) β

(c) λ (d) $F1$ score

Fig. 5. Real biological data using the data sets D1–D5.

surpass the PPV of the nonrigid method without z-score, but its TPR is much less than that of the nonrigid method without z-score regardless of the cut-off values of ω. The effect of both β and λ is significant for the nonrigid method with z-score. In both tuning parameters, the PPV of the method with z-score is larger than that of the method without z-score, while the TPR without z-score is larger than that with z-score.

The overall $F1$ scores are shown in Fig. 5(d). Although the absolute $F1$ scores are less than those of homogeneous cases (see Fig. 3(d)), the general trends are similar to each other. Namely, the rigid method without z-score has the largest variation, the nonrigid without z-score has the highest mean $F1$ score and other methods have the similar mean $F1$ scores to each other (see Table 1).

The one-way ANOVA and Tukey's post hoc analyses demonstrate that the nonrigid without z-score significantly achieves the highest mean $F1$ score among the four methods similar to the homogeneous cases (see Table 1). As can be seen in Table 2, the maximum $F1$ score occurs when the nonrigid method without z-score is used with $\omega = 0.999$, $\beta = 1$ and $\lambda = 1$.

4. Concluding Remarks

A new peak alignment method, PMA-PA, is developed using PMAs in order to deal with both homogeneous and heterogeneous GC×GC-MS data.

According to the application to the data sets A, B and C, the z-score standardization is necessary for heterogeneous cases but not for homogeneous cases in order to achieve the highest performance in peak alignment (Table 2), as we expected. The overall mean and maximum $F1$ scores demonstrate that the peak alignment will achieve the highest performance when the nonrigid method is utilized for both homogeneous and heterogenous data. This implies that the retention time shift is nonlinear. Note that, although the maximum $F1$ score is observed when the rigid method is used in homogeneous cases, the difference with the nonrigid method is not significant and further the overall mean $F1$ score of the nonrigid method is significantly higher than that of the rigid method (Table 1).

The developed algorithm was also validated using real biological data sets, which is a homogeneous case. This application further confirms that the nonrigid method without z-score performs the best among four methods in terms of the overall mean and maximum $F1$ scores. However, its optimal tuning parameters are different from those with the homogeneous data A. The optimal value of ω was larger with the data set D ($\omega = 0.999$) than that with the data set A ($\omega = 0$). In other words, the homogeneous data set A was aligned only based on a uniform distribution, while the biological homogeneous data set D was aligned dominantly based on GMM (see Eq. (2)). This is because the data set A has little shift in retention time. On the other hand, the optimal values of β and λ are smaller with the data set D than those with the data set A (Table 2). This is because the data set D is more dense than the data set A.

Table 3. The overall mean $F1$ score for each of pairwise peak alignment results using the one-way approach.

M	z	N	$F1$ score	N	$F1$ score	N	$F1$ score
		Homogeneous		Heterogeneous		Mice	
NR	No	54450	0.8860 (0.0002)	48400	0.0088 (0.0001)	12100	0.3522 (0.0004)
NR	Yes	54450	0.6525 (0.0004)	48400	0.5740 (0.0005)	12100	0.1690 (0.0007)
R	No	450	0.7288 (0.0102)	400	0.0121 (0.0010)	100	0.1635 (0.0173)
R	Yes	450	0.6521 (0.0043)	400	0.4970 (0.0047)	100	0.1504 (0.0080)

Note: 'M' stands for 'Method'; 'NR' and 'R' represent the nonrigid and rigid transformations, respectively; 'z' stands for the z-score standardization; 'N' is the total number of pairs considered; the numbers in parentheses represent the standard error.

On the basis of an anonymous reviewers suggestion, we also performed the PMA-PA using the one-way approach. In that case, instead of two PMA runs for the developed PMA-PA (i.e. two-way PMA-PA approach), we performed one PMA run and then used only the one-to-one matchings for the peak alignment. All the results of the one-way PMA-PA approaches are in Tables 3 and 4. As can be seen in Tables 1–4, the overall trends of the one-way PMA-PA are very similar to those of the two-way PMA-PA, but the overall $F1$ scores are higher in the two-way PMA-PA than in the one-way PMA-PA.

The z-score standardization can be considered as a nonrigid transformation so that one can expect that PMA-PA with nonrigid transformation would not be affected by z-score standardization, while PMA-PA with rigid transformation would

Table 4. The cases with the maximum $F1$ score for each of pairwise peak alignment results using the one-way approach.

M	z	N	ω	β	λ	TPR	PPV	$F1$ score
						Homogeneous		
NR	No	45	0	5	2.2	0.8453 (0.0087)	0.9719 (0.0041)	0.9035 (0.0062)
NR	Yes	45	0.999	1.8	1	0.7637 (0.0165)	0.9539 (0.0068)	0.8453 (0.0121)
R	No	45	0			0.8484 (0.0087)	0.9713 (0.0039)	0.9050 (0.0062)
R	Yes	45	0.999			0.7546 (0.0178)	0.9558 (0.0063)	0.8397 (0.0134)
						Heterogeneous		
NR	No	40	0.999	1	1	0.0095 (0.0022)	0.0386 (0.0089)	0.0152 (0.0035)
NR	Yes	40	0.889	2.6	4.6	0.6077 (0.0097)	0.9006 (0.0082)	0.7249 (0.0090)
R	No	40	0			0.0368 (0.0034)	0.1133 (0.0097)	0.0554 (0.0050)
R	Yes	40	0.999			0.4344 (0.0127)	0.7417 (0.0161)	0.5471 (0.0142)
						Mice		
NR	No	10	0.999	1	1	0.3615 (0.0157)	0.4422 (0.0135)	0.3974 (0.0145)
NR	Yes	10	0.999	5	5	0.2188 (0.0209)	0.2979 (0.0214)	0.2517 (0.0215)
R	No	10	0.111			0.1581 (0.0476)	0.2271 (0.0688)	0.1863 (0.0563)
R	Yes	10	0.999			0.2304 (0.0198)	0.3888 (0.0370)	0.2891 (0.0257)

Note: 'M' stands for 'Method'; 'NR' and 'R' represent the nonrigid and rigid transformations, respectively; 'z' stands for the z-score standardization; 'N' is the total number of pairs considered; the numbers in parentheses represent the standard error.

be. However, as shown in Table 2, the z-score standardization significantly contributes on the performances of both nonrigid and rigid transformations in case of heterogeneous data. On the other hand, the parameter estimation in PMA is carried out by EM algorithms which are known to be local optimization. One of disadvantages on local optimization is that the initial guess or starting value is critical and can greatly affect the outcome of the optimization. Thus, due to the nature of the data, the heterogeneous case will require a good initial guess enough to find a solution. Indeed, both nonrigid and rigid transformations yielded poor performance without z-score standardization, while the performance is dramatically improved with z-score standardization. In that regard, it seems that the z-score standardization provides a good initial guess for the heterogeneous data sets, resulting in a better performance in peak alignment.

All existing approaches use either both the peak (location) distance and the mass spectral similarities or only the mass spectral similarities, while the developed approach uses the peak distance only. For this reason, there is no available approach to compare with the proposed PMA-PA, except for one of the methods carried out in Ref. 7, which is PAD with Euclidean distance but only for homogeneous cases. Comparing with the results of PAD available in the Supplementary Data II of Ref. 7, PMA-PA performs better than PAD for both homogeneous and mice data sets (PMA-PA versus PAD: 93.61% versus 92.53% for homogeneous and 48.40% versus 47.28% for mice).

In conclusion, our applications to experiment data demonstrate that the points matching algorithm is promising for the peak alignment for both homogenous and heterogeneous data. In particular, in this study, we used only peak position or location information for the peak alignment different from the existing methods that use either both the peak (location) distance and the mass spectral similarities or only the mass spectral similarities. Although the peak location includes the less information than the mass spectral similarity, the developed PMA-based alignment achieves the comparable performances in terms of $F1$ scores.[6–8] In addition, this study shows that the nonrigid method is an optimal choice regardless of whether the data are homogeneous or heterogeneous.

Acknowledgments

This work was partially supported by the Grant No. DMS-1312603 from the National Science Foundation (NSF). The Biostatistics Core is supported, in part, by NIH Center Grant No. P30 CA022453 to the Karmanos Cancer Institute at Wayne State University.

References

1. Fraga CG, Prazen BJ, Synovec RE, Objective data alignment and chemometric analysis of comprehensive two-dimensional separations with run-to-run peak shifting on both dimensions, *Anal Chem* **73**:5833–5840, 2001.

2. Mispelaar VG, Tas AC, Smilde AK, Schoenmakers PJ, van Asten AC, Quantitative analysis of target components by comprehensive two-dimensional gas chromatography, *J Chromatogr A* **1019**:15–29, 2003.
3. Pierce KM, Wood LF, Wright BW, Synovec RE, A comprehensive two-dimensional retention time alignment algorithm to enhance chemometric analysis of comprehensive two-dimensional separation data, *Anal Chem* **77**:7735–7743, 2005.
4. Zhang D, Huang X, Regnier FE, Zhang M, Two-dimensional correlation optimized warping algorithm for aligning GCxGC-MS data, *Anal Chem* **80**:2664–2671, 2008.
5. Oh C, Huang X, Regnier FE, Buck C, Zhang X, Comprehensive two-dimensional gas chromatography/time-of-flight mass spectrometry peak sorting algorithm, *J Chr A* **1179**:205–215, 2008.
6. Wang B, Fang A, Heim J, Bogdanov B, Pugh S, Libardoni M, Zhang X, DISCO: Distance and spectrum correlation optimization alignment for two dimensional gas chromatography time-of-fligh mass spectrometry-based metabolomics, *Anal Chem* **82**:5069–5081, 2010.
7. Kim S, Fang A, Wang B, Jeong J, Zhang X, An optimal peak alignment for comprehensive two-dimensional gas chromatography mass spectrometry using mixture similarity measure, *Bioinf* **27**:1660–1666, 2011.
8. Kim S, Koo I, Fang A, Zhang X, Smith–Waterman peak alignment for comprehensive two-dimensional gas chromatography mass spectrometry, *BMC Bioinf* **12**:235, 2011.
9. Besl PJ, McKay ND, A method for registration of 3-D shapes, *in IEEE Trans Pattern Anal Mach Intell* **14**:239–256, 1992.
10. Gold S, Lu CP, Rangarajan A, Pappu S, Mjolsness E, New algorithms for 2D and 3D point matching: Pose estimation and correspondence, *Pattern Recognit* **31**:1019–1031, 1999.
11. Chui H, Rangarajan A, A new point matching algorithm for non-rigid registration, *Comput Vis Image Underst* **89**:114–141, 2003.
12. Myronenko A, Song X, Point set registration: Coherent point drift, *IEEE Trans Pattern Anal Mach Intell* **32**:2262–2275, 2010.
13. Girosi F, Jones M, Poggio T, Regularization theory and neural networks architectures, *Neural Comput* **7**:219–269, 1995.
14. Dempster A, Laird N, Rubin D, Maximum likelihood from incomplete data via the EM algorithm, *J R Stat Soc B, Methodol* **39**:1–38, 1977.
15. Rangarajan A, Chui H, Mjolsness E, Davachi L, GoldmanRakic PS, Duncan JS, A robust point matching algorithm for autoradiograph alignment, *Med Image Anal* **1**:379–398, 1997.
16. Wells WM, Statistical approaches to feature-based object recognition, *Int J Comput Vis* **22**:63–98, 1997.

Beichuan Deng is currently a Ph.D. candidate in Mathematics at Wayne State University (advised by Prof. Zhimin Zhang). He received his B.S. in Mathematics at Sichuan University (Sichuan, China) in 2013. His research is mainly about numerical methods for solving partial differential equations, especially fractional differential equations, including finite difference method, finite element method spectral method and their efficient algorithms.

Seongho Kim earned his B.S. in Mathematics at Chonnam National University (Gwangju, South Korea) in 1996 and his M.S. in Applied Mathematics in 2000 and Ph.D. in Applied Statistics in 2005 (with supervision of Prof. Sung-Ho Kim) at Korea Advanced Institute of Science and Technology (KAIST) (Daejeon, South Korea). He is currently an Assistant Professor in the Karmanos Cancer Institute (KCI) Biostatistics Core and in the Department of Oncology at Wayne State University School of Medicine. His research interests lie in the development of novel statistical methods and models for biological and clinical data including speech pattern recognition, decision support systems, comparative genomics/bioinformatics, cancer screening/diagnostics, pharmacokinetics/pharmacodynamics and metabolomics.

Hengguang Li received his B.S. degree in Computational Mathematics at Peking University, China in 2002 and his Ph.D. degree in Mathematics in 2008 at Penn State University. He is currently an Associate Professor in the math department at Wayne State University. His research is in the area of Applied Mathematics with main focus on Numerical Analysis, Partial Differential Equations, and Scientific Computing. His work reflects interplay of rigorous mathematical analysis of PDEs, the estimate and development of numerical methods, and their applications to physics, engineering and medicine.

Elisabeth Heath is an active scientific member of the Karmanos Cancer Institute (KCI) in Detroit, MI, USA. As Professor of Oncology and Medicine, her research focus is conducting clinical and translational research trials in genitourinary malignancies. She is the Director of Prostate Cancer Research and leads the Prostate Cancer Research Team (PCRT) at KCI. She has been successful in focusing the PCRT to conduct innovative, translational research in prostate cancer as well as fostering team science. She earned her medical degree from Thomas Jefferson University in Philadelphia, PA, USA, completed her internal medicine residency at Georgetown University Hospital, Washington, DC, USA, and completed her medical oncology fellowship at Johns Hopkins School of Medicine, Baltimore, MD, USA. She is a dedicated clinician, researcher and teacher at Wayne State University School of Medicine.

Xiang Zhang did his B.S. in Radiochemistry at the Lanzhou University (Lanzhou, China) in 1989 and his M.S. in Nuclear Physics at the Institute of Modern Physics, Chinese Academy of Sciences (Lanzhou, China) in 1992. He joined Purdue University (West Lafayette, IN) in 1996 and got his Ph.D. in Chemistry with supervision of Prof. Fred Regnier. Since 2008, he joined Department of Chemistry at the University of Louisville (Louisville, KY) where he is currently working as a Professor of Chemistry and the Director of Center for Regulatory & Environmental Analytical Metabolomics. His research interest is molecular systems biology, by exploiting practical and efficient high-throughput technologies for analyses of complex mixtures.